4-11-2017

Probabilistic performance-based design for high performance control systems

Laura Micheli
Iowa State University, lauramch@iastate.edu

Liang Cao
Iowa State University, liangcao@iastate.edu

Yongqiang Gong
Iowa State University, gongyq@iastate.edu

Alessandro Cancelli
Iowa State University, acancell@iastate.edu

Simon Laflamme
Iowa State University, laflamme@iastate.edu

See next page for additional authors

Probabilistic performance-based design for high performance control systems

Abstract
High performance control systems (HPCS) are advanced damping systems capable of high damping performance over a wide frequency bandwidth, ideal for mitigation of multi-hazards. They include active, semi-active, and hybrid damping systems. However, HPCS are more expensive than typical passive mitigation systems, rely on power and hardware (e.g., sensors, actuators) to operate, and require maintenance. In this paper, a life cycle cost analysis (LCA) approach is proposed to estimate the economic benefit these systems over the entire life of the structure. The novelty resides in the life cycle cost analysis in the performance based design (PBD) tailored to multi-level wind hazards. This yields a probabilistic performance-based design approach for HPCS. Numerical simulations are conducted on a building located in Boston, MA. LCA are conducted for passive control systems and HPCS, and the concept of controller robustness is demonstrated. Results highlight the promise of the proposed performance-based design procedure.

Keywords
structural control, high performance control systems, probabilistic performance-based design, life-cycle cost analysis, semi-active damping, variable friction

Disciplines
Civil Engineering | Controls and Control Theory | Structural Engineering | VLSI and Circuits, Embedded and Hardware Systems

Comments
This proceeding is published as Laura Micheli, Liang Cao, Yongqiang Gong, Alessandro Cancelli, Simon Laflamme, Alice Alipour, "Probabilistic performance-based design for high performance control systems", Proc. SPIE 10164, Active and Passive Smart Structures and Integrated Systems 2017, 101642I (11 April 2017); doi: 10.1117/12.2261449; doi:10.1117/12.2261449. Posted with permission.

Authors
Laura Micheli, Liang Cao, Yongqiang Gong, Alessandro Cancelli, Simon Laflamme, and Alice Alipour

Probabilistic performance-based design for high performance control systems

Laura Micheli, Liang Cao, Yongqiang Gong, Alessandro Cancelli, Simon Laflamme, et al.

Laura Micheli, Liang Cao, Yongqiang Gong, Alessandro Cancelli, Simon Laflamme, Alice Alipour, "Probabilistic performance-based design for high performance control systems," Proc. SPIE 10164, Active and Passive Smart Structures and Integrated Systems 2017, 101642I (11 April 2017); doi: 10.1117/12.2261449

SPIE.

Event: SPIE Smart Structures and Materials + Nondestructive Evaluation and Health Monitoring, 2017, Portland, Oregon, United States

Probabilistic Performance-Based Design for High Performance Control Systems

Laura Micheli[a], Liang Cao[a], Yongqiang Gong[a], Alessandro Cancelli[a], Simon Laflamme[a,b], and Alice Alipour[a]

[a]Department of Civil, Construction, and Environmental Engineering, Iowa State University, Ames, IA 50011, USA
[b]Department of Electrical and Computer Engineering, Iowa State University, Ames, IA 50011, USA

ABSTRACT

High performance control systems (HPCS) are advanced damping systems capable of high damping performance over a wide frequency bandwidth, ideal for mitigation of multi-hazards. They include active, semi-active, and hybrid damping systems. However, HPCS are more expensive than typical passive mitigation systems, rely on power and hardware (e.g., sensors, actuators) to operate, and require maintenance. In this paper, a life cycle cost analysis (LCA) approach is proposed to estimate the economic benefit these systems over the entire life of the structure. The novelty resides in the life cycle cost analysis in the performance based design (PBD) tailored to multi-level wind hazards. This yields a probabilistic performance-based design approach for HPCS. Numerical simulations are conducted on a building located in Boston, MA. LCA are conducted for passive control systems and HPCS, and the concept of controller robustness is demonstrated. Results highlight the promise of the proposed performance-based design procedure.

Keywords: structural control, high performance control systems, probabilistic performance-based design, life-cycle cost analysis, semi-active damping, variable friction

1. INTRODUCTION

The use of high strength materials and advanced structural systems produces lighter and more flexible structures. Some of these structures, in particular tall buildings, are more prone to wind-induced vibrations. Wind-induced vibrations can result in considerable non-structural damages and excessive accelerations. While non-structural damages can provoke injuries and important economic losses, excessive accelerations can interfere with the occupants daily activities. A solution is to increase structural performance versus motion by sizing structural stiffness and integrating damping system, also known as performance-based design (PBD).[1]

The PBD approach consists of designing structural dynamic parameters to restrict motion to a prescribed level of performance for given hazards. This is typically done through the design of stiffness elements and the utilization of passive energy dissipation systems. However, such approach is usually tuned to a specific hazard and can be ineffective to mitigate other events. High-performance control systems (HPCS) have been proposed as an alternative. Examples of HPCS including variable fluid, variable stiffness, variable orifice, and variable friction mechanisms can be found in Refs.[2–6] HPCS include active, semi-active and hybrid damping systems, and are capable of adaptive actions in a controlled manner, therefore providing performance over a wide excitation bandwidth.[7] Several studies demonstrated that integrating HPCS in a structural system may lead to savings on materials[8,9] and decrease of life-cycle cost of structures.[10–12]

Despite such demonstrated promise, HPCS are yet to be widely accepted and implemented. A strategy to improve on the acceptability of HPCS is to account for economic benefits and demonstrate their economic savings over the structure's life cycle. This is typically done through life-cycle analysis (LCA),[13] in particular for wind excitations.[14] However, there are few examples in literature on LCA being applied to supplemental damping system.[15] Among such examples, Wen and Shinozuka[16] studied the cost-effectiveness of an active control system. A LCA has been conducted on a controlled structure, followed by a cost-benefit analysis of the control system that included the initial cost of actuators and cost of maintenance. Cases of linear and nonlinear actuation were analyzed for a structure subjected to earthquakes. Hahm *et*

Further author information: (Send correspondence to Liang Cao)
Liang Cao: E-mail: liangcao@iastate.edu, Telephone: 1 716 472 6595

Active and Passive Smart Structures and Integrated Systems 2017, edited by Gyuhae Park, Alper Erturk, Jae-Hung Han, Proc. of SPIE Vol. 10164, 101642I
 · doi: 10.1117/12.2261449

al.[17] studied the impact of semi-active dampers on the life-cycle cost of a long span bridge subjected to earthquake loads. These examples of LCA of HPCS are specific to seismic events. Takahashi *et al.*[15] demonstrated that the estimated cost of a structure with passive dampers was significantly lower in comparison to a bare frame. Gidaris & Taflanidis[18] proposed a procedure for the optimal design for viscous damper systems for seismic applications based on the minimization of the life-cycle cost. Although some studies have developed PBD approaches for structure under wind events,[19–22] the integration of the LCA in a PBD for HPCS has never been investigated. Note that multi-level wind hazards refer to wind event with various intensities (e.g., moderate-to-high winds and extreme winds).

In this paper, a LCA procedure for structures equipped with HPCS and exposed to multi-level winds is presented. The objective is to provide a procedure enabling the holistic integration of these devices during the structural design stage, with a particular focus on wind-induced vibrations. The design approach consists of establishing performance criteria for wind-induced vibrations, conducting a life-cycle analysis (LCA) to quantify the overall benefits of the structural system equipped with HPCS, and comparing the economic performance with respect a cost thresholds. Structural performance versus motion is not directly verified through the structure's response, but is embedded in the life cycle cost.

The rest of the paper is organized as follows. Section 2 presents the PBD framework for structures exposed to wind hazards. It includes the integration HPCS design and the LCA model. Section 3 demonstrates the PBD procedure on a simulated 39-story structure. The HPCS of interest is a based on a Banded Rotary Friction Device (BRFD) previously proposed by the authors.[6] Section 4 presents simulation results and perform LCA to investigate the economic viability of the HPCS. Section 5 concludes the paper.

2. PERFORMANCE-BASED DESIGN FOR WIND HAZARDS

The proposed PBD procedure for structures equipped with HPCS and exposed to mutli-level wind hazards is schematized in Fig. 1. First, the design wind loads are established based on codes and other considerations (e.g., wind tunnel tests), followed by the PBD performance objectives. Then, the HPCS is designed and the LCA is performed. The LCA returns a life cycle cost (LCC), and its value is compared against a general cost performance function that represents the economic performance threshold. If the LCC is lower than the cost performance function, then the design is satisfied, otherwise the design of the HPCS is to be altered. This section discusses the performance objectives and LCA procedure.

2.1 Performance Objectives

The main interest in this study is acceleration. While acceleration is mostly related to serviceability, it may result in non-structural damage when excessive. The ASCE/SEI 7-10 (2013)[23] does not define specific performance limits for wind excitations and the serviceability verification is usually left to the designer. Efforts have been conducted to define maximum acceptable acceleration thresholds[24,25] in order to minimize motion sickness and fatigue, drowsiness, and mood changes from prolonged motion (i.e., the sopite syndrome). Griffis[26] reported on various thresholds proposed for residential and office buildings. Mendis *et al.*[27] gave specific guidelines on general human perception thresholds and described discomfort related to different levels of acceleration, as listed in Table 1.

Table 1: Acceleration thresholds for human discomfort[27] adopted for the PPBD approach

threshold (mg)	discomfort description
$\leq$25.0	motion well perceivable; vibrations can influence desk work and cause motion-sickness if repeated for long time
25.0−50.0	majority of people strongly perceive the motion and experience difficulties in desk work; possibility of losing balance
50.0−70.0	intolerable motion and difficulties to walk
>90.0	intolerable threshold

Here, the authors propose a PBD objective matrix for structures subjected to wind excitation. The matrix is presented in Fig. 2. The acceleration thresholds are based on those suggested in Ref.[27] as listed in Table 1. They are associated with four wind mean recurrence intervals (MRI). Three general performance objectives are defined: basic, essential and critical performance. The basic performance objective corresponds to the design level that the majority of buildings should

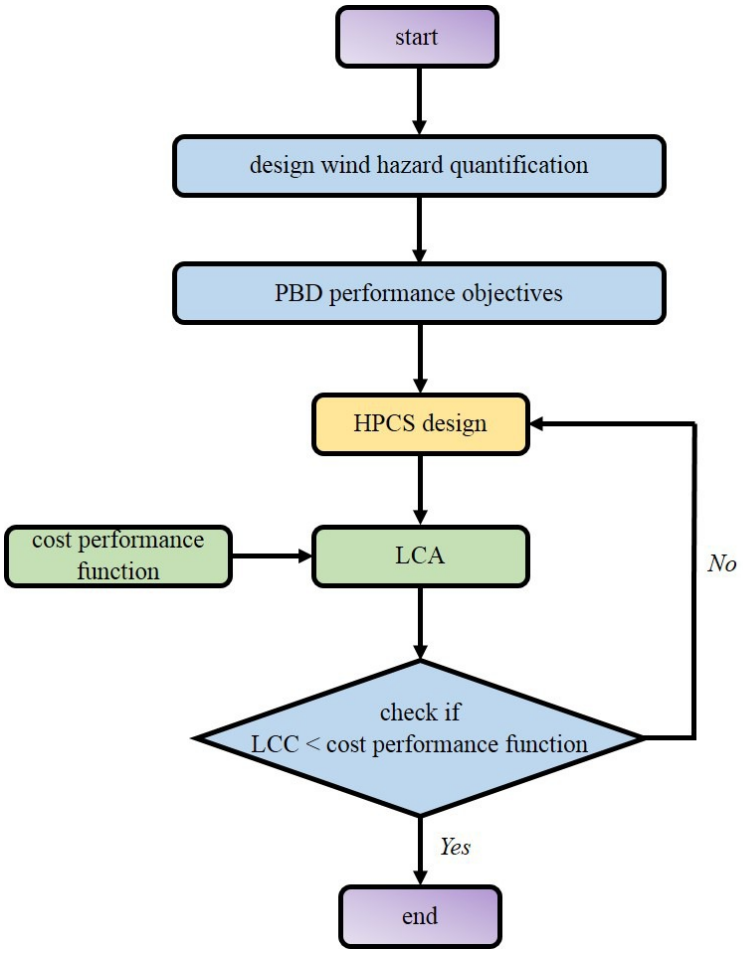

Figure 1: Proposed PBD procedure for HPCS used in wind hazard mitigation

satisfy to ensure serviceability during daily operations. The critical performance objective is used for buildings that must remain fully functional during extreme events. Examples of such buildings include hospitals and strategic governmental buildings. In between is the essential performance criteria, which is often associated with specialized structures, such as chip manufactures and certain research laboratories, that require tighter acceleration thresholds to maintain operations. The acceleration thresholds associated with each performance objective are relaxed with increasing wind hazard levels. For instance, during extreme wind (475 years MRI), the extreme maximum acceleration threshold is acceptable under the basic performance objective.

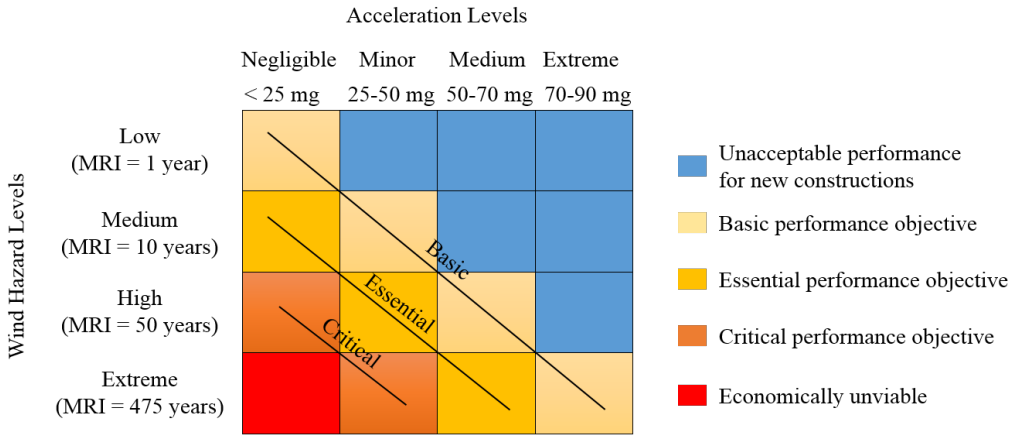

Figure 2: Performance-based matrix for wind excitations

2.2 Life Cycle Cost Analysis

The LCA is based on the expected LCC function defined in Eq. 1.

$$\mathrm{LCC} = C_0 + C_f \tag{1}$$

where C_0 denotes the initial construction cost and C_f is the cost associated with discomfort and frequent inoperability, expressed as

$$C_f = \sum_{i=1}^{N_t} \sum_{y=1}^{k} C_y P_y (1+r)^{-i\Delta t} \tag{2}$$

where Δt is the time interval (= one year), N_t is the number of time periods considered (= the design life of the structure), r is the expected rate of return (=5%),[13] k is the number of considered acceleration levels at the i^{th} time period, P_y is the probability of the y^{th} acceleration level to occur, and C_y is the economic loss associated with the y^{th} acceleration level being exceeded. P_y can be determined by:[28]

$$P_y = \int_{V_{d,\min}}^{V_{d,\max}} p_y(V_d)\, p_w(V_d)\, dV_d \tag{3}$$

where V_d is the design mean wind speed at 10 m above the ground, selected as engineering demand parameter, varying between the minimum and maximum mean wind levels $V_{d,\min}$ and $V_{d,\max}$, respectively, $p_y(V_d)$ denotes the probability of the y^{th} acceleration level occurring under the wind speed V_d, and $p_w(V_d)$ is the wind speed hazard function that represent the probability of V_d exceeding the time period. Parameters $V_{d,\min}$ and $V_{d,\max}$ are user-defined based on the building location and the wind velocities that the structure is likely to experience during its life span. The method to determine parameters p_y and p_w are described in Section 4.2.

3. METHODOLOGY

A 39-story office tower located in downtown Boston, MA, is simulated to evaluate the proposed PBD procedure. It is modeled along its weak axis as a lumped-mass shear system using the dynamic parameters reported in Ref.[29] The weak direction of the structure was selected because it corresponded to the largest acceleration response reported in Refs.[12,30] The structure is currently equipped with passive viscous dampers, installed to mitigate wind-induced vibrations. The existing configuration will be used to benchmark performance of the HPCS. This passive system, along with the simulated HPCS, are described in the upcoming subsection. The subsequent subsection presents the methodology used for generating wind loads.

3.1 Simulated control cases

The simulated controlled cases include the passive viscous case - the structure with its existing damper configuration; the HPCS case - the viscous dampers are replaced with variable friction devices (BRFD); and the passive-on - the BRFD used passively with full power. The performance of each control case is benchmarked against the uncontrolled case, which consists of the existing structure without its viscous dampers.

Passive viscous case

The current passive configuration consists of passive fluid viscous dampers installed at every other floor. They were installed to mitigate wind-induced vibrations produced by vortex shedding from a nearby 52-story building. The viscous dampers are installed from the 5th floor and up. They have a capacity of 1350 kN below the 26th floor and of 900 kN above 26th floor, with a damping coefficient of 52550 $kN \cdot s/m$ and 35000 $kN \cdot s/m$, respectively, as listed in Table 2. The simulated dampers are installed at the same locations as the passive system, installed in a diagonal bracing element.

Table 2: Viscous damping properties

floor	c_j $(kN \cdot s/m)$	capacity (kN)	number
below 26th floor	52550	1350	22
above 26th floor	35000	900	8

HPCS case

The HPCS of interest is based on the BRFD presented by the authors in Ref.[6] Its mechanical principle is based on a band brake, which results in a high amplification of the applied force while enabling a variable control force. Its dynamics has been characterized and simulated.[6,7] Figures 3 (a) and (b) are plots of modeled force-displacement and force-velocity loops from a characterized 45 kN capacity prototype BRFD as a function of actuation force capacity (13%, 20%, 25%,50% and 100%). Here, BRFD dynamics will be scaled to match the design capacity. The BRFD are installed in the same floor as the passive viscous case and its design capacity is taken as 900 kN, the minimum damping capacity of all the viscous dampers. Simulation results will show that such placement strategy for the HPCS provides similar damping capacity under the passive-on case compared with the viscous damping system.

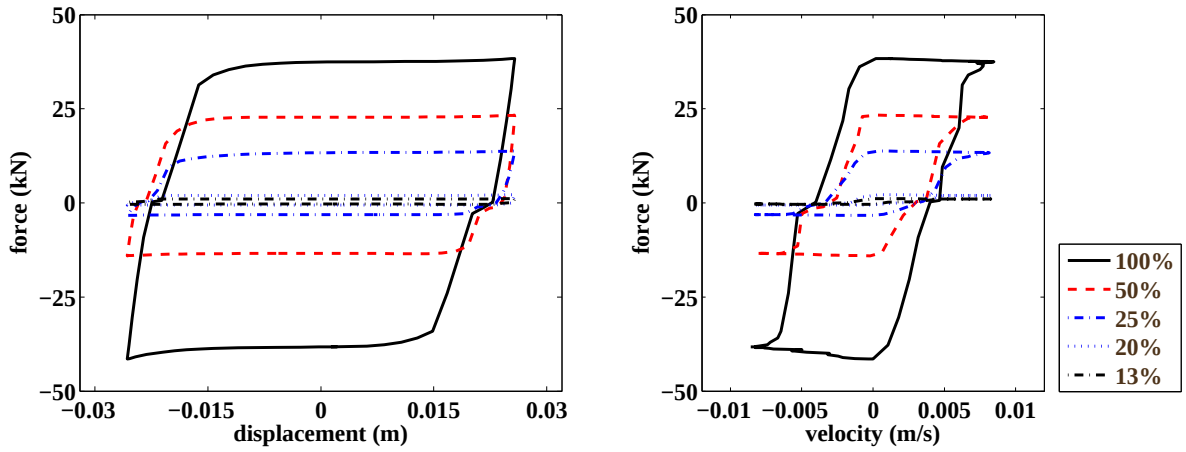

(a) (b)

Figure 3: Modeled dynamics of the BRFD under various applied forces under a 0.05 Hz excitation of 25.4 mm (1 in) amplitude: (a) force-displacement; (b) force-velocity

An LQR controller is used to compute the required damping force F_{req}, and the BRFD receives to attempt to generate F_{req}. A linear voltage delay is induced in the actuator:

$$\dot{v}_{\text{act}} = -\tau(v_{\text{act}} - v_{\text{req}}) \tag{4}$$

where v_{req} and v_{act} are required and actual voltage; and τ is a positive delay constant taken as $\tau = 200\ \text{sec}^{-1}$ to be consistent with the value reported in Ref.[12]

Passive-on case

The passive-on case refers to the BRFD using full voltage, continuously.

Here, a single performance objective is selected, consisting of the maximum absolute acceleration response J_a during an excitation, and the thresholds are consistent with the PBD matrix (Fig. 2): the corresponding maximum acceleration threshold for four wind hazard level are 25, 50, 70 and 90 mg. In addition, in order to assess the performance of the damping devices,

$$J_a = \frac{\max_{i,t}|\ddot{x}_{\text{unc},i}(t)| - \max_{i,t}|\ddot{x}_i(t)|}{\max_{i,t}|\ddot{x}_{\text{unc},i}(t)|} \tag{5}$$

where $\ddot{x}_{\text{unc},i}(t)$ represents the acceleration of i^{th} floor at time t for the uncontrolled case, while $\ddot{x}_i(t)$ is the absolute acceleration under a controlled case.

3.2 Wind loads

Wind loads are generated for the simulation using the following methodology. The time series of a wind speed at the j^{th} floor are taken as:

$$V_{w,j}(t) = V_{d,j} + V_{g,j}(t) + V_{r,j}(t) \tag{6}$$

where $V_{d,j}$ is the design average wind speed, $V_{g,j}(t)$ is a sinusoidal wind gust that represents vortex shedding produced by the nearby building:

$$V_{g,j}(t) = \begin{cases} 0 & \text{if} \quad t < T_{\text{sg}} \\ \bar{V}_{g,j}\sin(\omega_g t) & \text{if} \quad T_{\text{sg}} < t < T_{\text{eg}} \\ 0 & \text{if} \quad t > T_{\text{eg}} \end{cases} \tag{7}$$

where T_{sg} and T_{eg} are the start and end time of the gust, respectively, $\bar{V}_{g,j}$ is the gust amplitude, ω_g is gust frequency, taken as the natural frequency of building, and $V_{r,j}(t)$ is the time series of wind turbulence coupled with the wind turbulence acting on other floors. Time series $V_{r,j}(t)$ is constructed from a power spectral density matrix $\mathbf{S}(\omega)$:[31]

$$\mathbf{S}(\omega) = \begin{bmatrix} S_{11}(\omega) & S_{12}(\omega) & \cdots & S_{1N}(\omega) \\ S_{21}(\omega) & S_{22}(\omega) & \cdots & S_{2N}(\omega) \\ \vdots & \vdots & \ddots & \vdots \\ S_{N1}(\omega) & S_{N2}(\omega) & \cdots & S_{NN}(\omega) \end{bmatrix}_{N\times N} \tag{8}$$

where N is the number of floors, ω is the frequency (rad/s), and each element of the power density matrix $S_{jl}(\omega)$ is expressed as:

$$S_{jl}(\omega) = \begin{cases} s_j(\omega) & j = l \\ \sqrt{s_j(\omega)s_l(\omega)}\gamma_{jl}(\omega) & j \neq l \end{cases} \tag{9}$$

where $\gamma_{jl}(\omega)$ is the coherence function between the j^{th} floor and the l^{th} floor, and $s_j(\omega)$ is the power spectral density value at the j^{th} floor of height h_j:

$$\gamma_{jl}(\omega) = \exp\left[-\frac{10\omega|h_j - h_l|}{\pi(V_{d,j} + V_{d,l})}\right] \tag{10}$$

$$s_j(\omega) = \frac{50u_*^2 h_j}{\pi V_{d,j}\left[1+\frac{25\omega h_j}{\pi V_{d,j}}\right]^{5/3}} \tag{11}$$

with the shear velocity of wind flow u_*:

$$u_* = \frac{0.4V_{d,j}}{\ln(h_j/z_b)} \tag{12}$$

The power density matrix $\mathbf{S}(\omega)$ is decomposed into:

$$\mathbf{S}(\omega) = \mathbf{H}(\omega)\mathbf{H}^{T*}(\omega) \tag{13}$$

where the asterisk denotes the complex conjugate and $H(\omega)$ is a lower triangular matrix of the form

$$\mathbf{H}(\omega) = \begin{bmatrix} H_{11}(\omega) & 0 & \cdots & 0 \\ H_{21}(\omega) & H_{22}(\omega) & \cdots & 0 \\ \vdots & \vdots & \ddots & \vdots \\ H_{N1}(\omega) & H_{N2}(\omega) & \cdots & H_{NN}(\omega) \end{bmatrix}_{N\times N} \tag{14}$$

The time series of wind turbulence at j^{th} floor can be obtained using:[31]

$$V_{r,j}(t) = 2\sum_{m=1}^{j}\sum_{q=1}^{N_\omega} |H_{jm}(\omega_{mq})|\sqrt{\Delta\omega}\cos[\omega_{mq}t - \theta_{jm}(\omega_{mq}) + \Phi_{mq}] \tag{15}$$

where $\Delta\omega$ is a frequency step amplitude; Φ_{mq} is a random phase uniformly distributed between 0 and 2π; $\theta_{jm}(\omega_{mq})$ is written as:

$$\theta_{jm}(\omega_{mq}) = \tan^{-1}\frac{Im[H_{jm}(\omega_{mq})]}{Re[H_{jm}(\omega_{mq})]} \tag{16}$$

In Eq. 15, the frequency spectrum of wind turbulence is equally spaced by N_ω frequency points of cut-off frequency $\omega_u = N_\omega\Delta\omega$. The frequency ω_{mq} is taken as:

$$\omega_{mq} = q\Delta\omega - \frac{j-m}{j}\Delta\omega \tag{17}$$

Finally, the wind load $F_{w,j}$ acting on the j^{th} floor of the building is given by:[32]

$$F_{w,j} = \rho c_D A_j V_{d,j}(V_{r,j}(t) + V_{g,j}(t)) \tag{18}$$

where ρ is the air density ($\rho = 1.225kg/m^3$, at 15 °C and standard atmospheric pressure); c_D is the drag coefficient (c_D is taken as 1.5[33]); A_j is the area exposed to the wind flow.

Four levels of wind hazard are considered in the simulations: 1, 10, 50 and 475 years MRI. Table 3 reports the average wind speed values V_d (m/s) at a height of 10 m for example.

Table 3: Design average wind speed V_d values

wind hazard level	MRI (year)	V_d (m/s)
low	1	14.0
medium	10	19.0
high	50	23.0
extreme	475	28.0

For each wind hazard level, six wind load time series of 10 minutes were produced. The wind load generation parameters are listed in Table 4. Fig. 4 shows a typical wind speed and wind load time series at the 36th floor for the extreme wind hazard level.

Table 4: Parameter values in $V_g(t)$ and $V_r(t)$

parameter	value	unit
$\bar{V}_g$	0.7	m/s
T_{sg}	150	s
T_{eg}	300	s
z_b	0.3	m
ω_u	2	Hz
ω_g	5.26	Hz
N	39	NA
k_v	0.4	NA
N_ω	2^{12}	NA

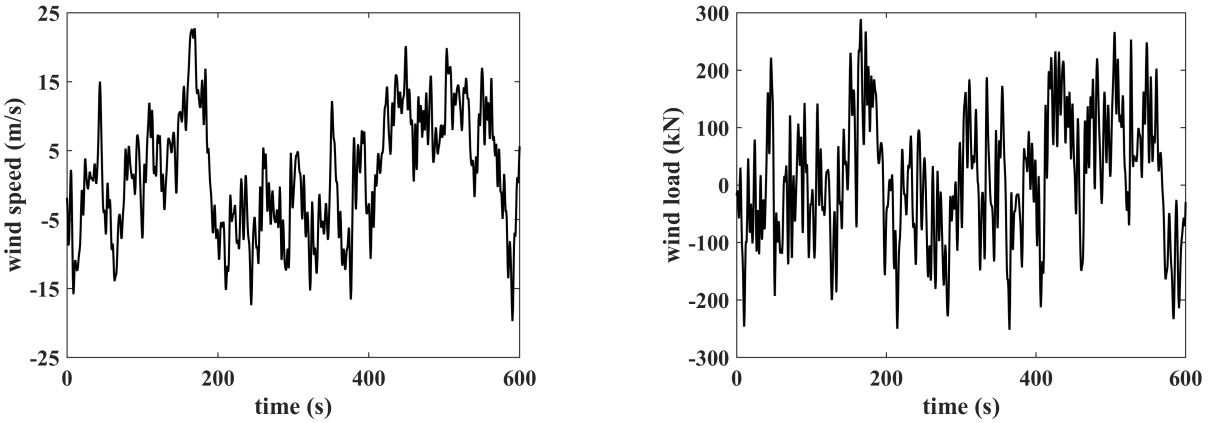

(a) (b)

Figure 4: The extreme wind hazard level at 36th floor: (a) time series of wind speed $V_{w,36}(t)$; and (b) time series of wind drag force $P_{w,36}(t)$.

4. RESULTS

Each control case is simulated under four wind hazard levels, and each wind hazard level is simulated under six different wind time series realizations and results averaged. In what follows, we simulate structural response under these wind hazards, and perform LCA to assess the economic viability of the HPCS.

4.1 Structural Responses

Table 5 lists the maximum acceleration results and values of J_a from simulations, and includes the average number of floors N_f in which the acceleration threshold was exceeded. These results show that only the HPCS successfully mitigate all wind hazard levels which could be attributed to its high control reachability. On the other hand, the passive-on and viscous cases provide great performance for the small, medium, and large wind hazard levels. A further inspection of results shows that the HPCS underperforms the passive-on and viscous cases in terms of maximum acceleration for the small and medium wind hazard levels. This can be attributed to the substantially low displacement of the control devices resulting in a low control reachability. A comparison of performance between the passive-on and viscous cases shows that the HPCS performs similarly to the viscous system if used passively.

Table 5: Simulation results under four wind hazard levels

wind hazard level	vibration threshold (mg)	control case	maximum acceleration (mg)	J_a (%)	N_f
low	≤ 25	HPCS	24.9	24.7	0
		passive-on	22.0	33.6	0
		viscous	20.9	36.9	0
		uncontrolled	33.1	NA	8
medium	$25-50$	HPCS	42.0	30.3	0
		passive-on	39.9	33.8	0
		viscous	37.7	37.5	0
		uncontrolled	60.2	NA	6
high	$50-70$	HPCS	56.4	40.0	0
		passive-on	60.0	36.2	0
		viscous	59.6	36.6	0
		uncontrolled	94.0	NA	9
extreme	$70-90$	HPCS	88.6	36.7	0
		passive-on	94.9	32.2	2
		viscous	94.7	32.3	2
		uncontrolled	140.3	NA	13

4.2 Life cycle Analysis

To conduct the LCA procedure, it is necessary to quantify the annual economic loss C_y in Eq. 2. In this study, the values suggested by Lamb and Kwok[25] were taken as reference. More specifically, it is assumed that 5.4 % of the employees working on the top one third floors ($26^{\text{th}}-36^{\text{th}}$ floor) of the building are affected from sopite syndrome or motion sickness when the maximum floor acceleration reached beyond 25 mg, with a consequent mean reduction in working performance of 30% per employee. Note that the top three floors ($37^{\text{th}}-39^{\text{th}}$ floor) are not considered in this study since those floors are not occupied. The total floor area of our simulated building is 2090 m^2.[30] Based on the standard office dimensions and the dimension of the simulated building, the total number of workers is estimated as 15300 people, with an average of 425 workers per floor assumed. The average annual salary for each employee is estimated based on the US National Occupational Employment and Wage Estimates[34] and taken as US$112,500. Furthermore, the average salary per day for each employee is calculated as US$477 assuming 235 work days per year, yielding a loss in productivity per person of US$143 per day. Details of life cycle components for the simulated building are listed in Table 6.

Table 6: Estimated life cycle components for the simulated building

element	value
floor area	2090 m^2
employees per floor	425
employees on the top 1/3 floors ($26^{\text{th}}-36^{\text{th}}$)	4250
average annual salary	USD $112,500
average salary per day	USD $477
economic loss per employee per day	USD $143

4.2.1 Fragility Analysis

Probability P_y in Eq. 3 is determined through $p_y(V_d)$ from a fragility analysis. It is assumed that the building fails ($p_y(V_d) = 1$) if at least one floor's maximum acceleration exceeds the y^{th} acceleration level under design mean wind speed V_d. Otherwise, the $p_y(V_d)$ is set to 0. The fragility analysis is conducted under design mean wind speeds ranging between $V_{d,\min}$ and $V_{d,\max}$, which represent the wind events that the structure will most likely experience during its life (N_t = 50 years). Here, $V_{d,\min}$ and $V_{d,\max}$ are taken as 22 m/s and 55 m/s, respectively, which range covers the design mean wind speed from low to extreme wind events at the average height of the last top third floors ($h = 130m$).

For each y^{th} acceleration level, a continuous fragility curve is generated from discrete data p_y to obtain P_y. Typically, $p_y(V_d)$ is estimated by a log-normal function, characterized by a log-standard deviation χ and a median μ:[13]

$$p_y(V_d;\chi,\mu) = \Phi_{\text{nor}}\left[\frac{\ln(V_d/\mu)}{\chi}\right] \tag{19}$$

where $\Phi_{\text{nor}}[\cdot]$ represents the standard normal distribution function. Parameter values of χ and μ are calculated by the maximum likelihood estimation (MLE) method based on simulation results. To avoid any intersection between the curves, only one value of log-standard deviation χ is set for all the acceleration levels.[13] Table 7 reports the estimated values of medians μ and the log-standard deviations χ for the semi-active and uncontrolled cases. Note that the value of μ for the uncontrolled case under the 25 mg acceleration level is set to 1 since this threshold is always exceeded. The estimated continuous probability function p_y for extreme acceleration level under HPCS, passive viscous, and uncontrolled cases are plotted in Fig.5.

Table 7: Parameter values of the fragility curves

	log-standard deviation μ				median
case	25 mg	25-50 mg	50-70 mg	70-90 mg	χ
HPCS	1.00	3.20	3.26	3.32	0.09
viscous	3.15	3.29	3.34	3.38	0.10
uncontrolled	3.13	3.28	3.36	3.41	0.12

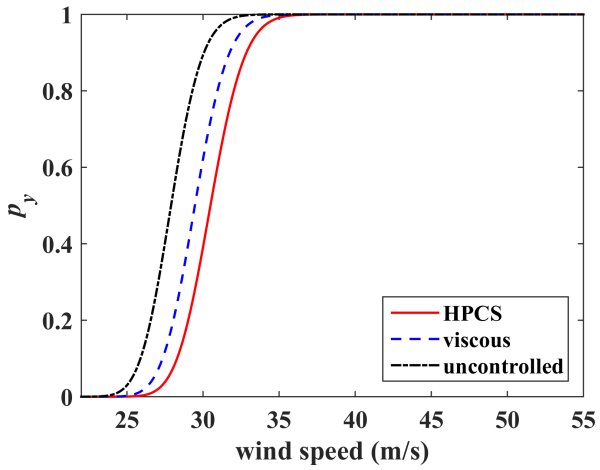

Figure 5: Estimated probability p_y for extreme acceleration level

4.2.2 Hazard Curve

For a realistic representation of the wind speed hazard curve $p_w(V_d)$, climatological annual data from 1984 to 2015 are taken from the National Oceanic and Atmospheric Administration (NOAA)[35] at the building's site (Boston, MA, Station 44013), and fitted with a probabilistic distribution function. The maximum annual wind speed data at a height $h = 5$ m above the open sea level are extracted and converted to the building location terrain. The discrete wind speed data are analyzed and fitted with the MLE method by a three parameters Weibull probability density function to obtain the continuous wind speed hazard function $p_w(V_d)$:

$$p_w(V_d;\eta,\beta,\gamma) = \frac{\beta}{\eta}\left(\frac{V_d-\gamma}{\eta}\right)^{\beta-1}\exp\left[\left(\frac{V_d-\gamma}{\eta}\right)^{\beta}\right] \tag{20}$$

where $\beta = 0.07$ is the shape parameter, $\eta = 3.0$ is the scale parameter and $\gamma = 20.1$ is the location parameter. The wind speed hazard function p_w at the average height of top one third floors ($h = 130$ m) is plotted in Fig. 6.

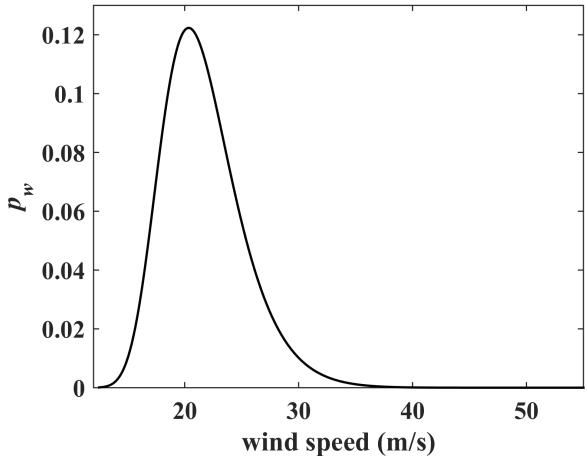

Figure 6: Wind speed hazard function p_w at height $h = 130$ m

4.3 Simulation Results

The resulting probabilities P_y under the various acceleration levels are listed in Table 8.

Table 8: P_y (%) under various acceleration levels

acceleration level	uncontrolled	viscous	HPCS
negligible	99.35	32.5	35.83
minor	20.85	11.34	11.34
medium	10.84	5.06	4.13
extreme	4.90	2.41	1.41

It is assumed that higher levels of acceleration correspond to higher percentages of building occupants affected by motion sicknesses (maintaining the loss of work productivity at 30%). Four different scenarios of functions linking the percentage of building occupants affected from motion sickness ρ_p and the maximum acceleration levels $\max(\ddot{x})$ are investigated. All cases start with the assumption that 5.4% of workers will suffer from motion sickness when the maximum acceleration reaches $\max(\ddot{x}) = 25$ mg based on Ref.[25] In linear-1 case, it is assumed that 100% of employees cannot tolerate acceleration beyond the extreme level ($\max(\ddot{x}) = 90$ mg) and a linear function is used to interpolate ρ_p between 25 and 90 mg. The linear-2 case assumes a linear proportional relationship for increasing levels of acceleration. In the convex case, it is assumed that 70% of employees will be affected when $\max(\ddot{x}) = 90$ mg (extreme level) and an arbitrary convex function ($\rho_p = 73.8\exp(232.3\max(\ddot{x}))$) is used. Lastly, the concave case assumes that 100% of employees cannot work beyond the medium level of acceleration ($\max(\ddot{x}) = 70$ mg) and uses an arbitrary concave relationship ($\rho_p = 91.8\ln(\max(\ddot{x}))$+290.3). For all cases, it is assumed that a motion is felt at least once a month for a total of 12 times per year.[24] The annual economic losses C_y associated with each relationship $\rho_p - \max(\ddot{x})$ are listed in Table 9.

Table 9: Annual economic losses C_y under various acceleration levels and relationship between ρ_p and $\max(\ddot{x})$

	annual economic loss C_y			
acceleration level	linear-1	linear-2	convex	concave
negligible	\$394,680	\$394,680	\$394,680	\$394,680
minor	\$3,047,616	\$787,644	\$1,055,340	\$5,039,892
medium	\$5,170,308	\$1,103,388	\$2,318,316	\$7,293,000
extreme	\$7,293,000	\$1,419,132	\$5,098,236	\$8,978,112

The cost-effectiveness of the HPCS strategy is compared against that of the viscous system (the passive-on case is not considered) using the LCC values. An installation cost of USD\$10,000 per BRFD (which includes the BRFD device,

bracing, and a lumped maintenance cost) and of USD$5,000 per viscous damper were assumed.[29] The resulting LCC values are marked in Fig. 7 under various acceleration effect scenarios. The difference between LCC (HPCS) and LCC (viscous) is the cost-effectiveness metric for the HPCS, listed in Table 10 (HPCS gain versus viscous). LCC results demonstrate that the HPCS strategy offers a remarkable economic gain in comparison to the viscous case when more employees are affected from wind-induced motion sickness (linear-1 and concave cases). This is attributed to the HPCS's mitigation performance relative to the viscous dampers being better for higher acceleration levels. The economic benefits of HPCS relative to the viscous system becomes insignificant when fewer employees have motion sickness under high acceleration (linear-2 and convex cases). For completing the analysis, the cost performance function (or LCC threshold) is taken as the LCC value of the uncontrolled structure. Results are listed in the Table 10, with the HPCS economic gain versus the uncontrolled and viscous cases. For all cases, the HPCS provides an certain economic advantage, which economic advantage increases with the increase of employees affected by higher acceleration. It can also be observed that both control systems offer a notable economic gain versus the uncontrolled case (viscous gain not shown in Table 10. Remark: while this analysis offers an economic justification for the installation of control systems (either passive systems or HPCS), the decision to equip the building with the existing viscous system arose from technical metrics, where it was found through wind tunnel tests that the uncontrolled structure would exceed acceptable acceleration thresholds.

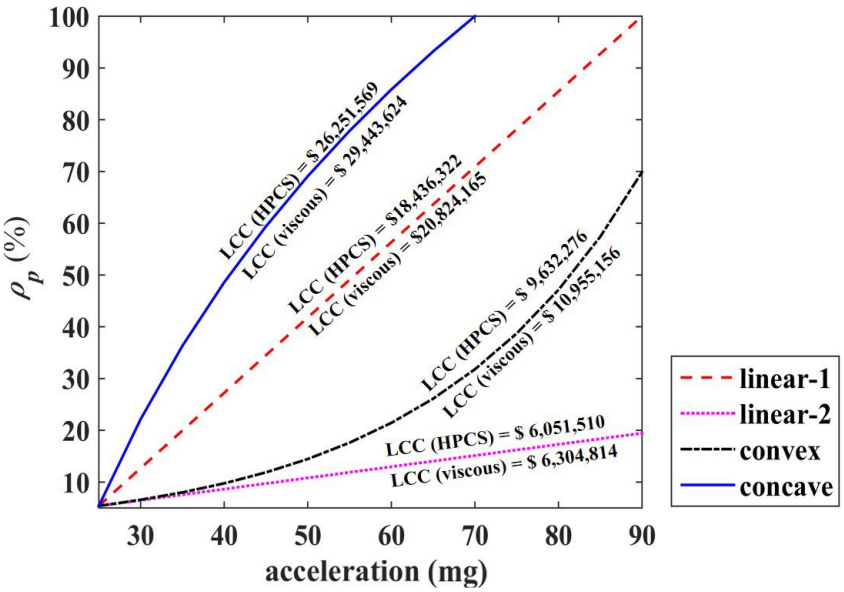

Figure 7: Assumed relationships between ρ_p and $\max(\ddot{x})$ and associated LCC values

Table 10: LCC and cost performance function values for various relationships between ρ_p and $\max(\ddot{x})$

	LCC		cost performance function	HPCS gain vs	
case	HPCS	viscous	uncontrolled	uncontrolled	viscous
linear-1	$18,436,322	$20,824,165	$37,255,178	-$18,818,856	-$2,387,843
linear-2	$6,051,510	$6,304,814	$10,993,619	-$4,942,109	-$253,304
convex	$9,632,276	$10,955,156	$19,540,410	-$9,908,134	-$1,322,880
concave	$26,251,569	$29,443,624	$52,562,375	-$26,310,806	-$3,192,055

5. CONCLUSION

This paper introduced a novel performance-based design (PBD) methodology for structures equipped with high-performance control systems (HPCS) exposed to multi-level wind excitations. In the proposed PBD procedure, the HPCS is first sized from quantified design wind hazards and established performance metrics as a function of the wind hazard levels and design objective. A life cycle analysis is performed to obtain life cycle cost values for the HPCS, which values are compared

against an economic threshold termed the cost performance function. If the HPCS provides an economic benefit, then the design is successful, otherwise the HPCS is re-designed. Such PBD strategy enables the incorporation of controllers in the analysis and other components of the closed-loop system.

The PBD procedure was demonstrated vis numerical simulations on an existing 39-story building, located in Boston (MA). The structure is currently equipped with viscous dampers to mitigate wind accelerations. The simulations investigated a virtual replacement of the viscous dampers with a variable friction device termed Banded Rotary Friction Device (BRFD). The BRFD was controlled by an LQR controller and included a voltage delay. The objective of the simulation was to show that an advanced control system could provide a certain economic benefit in comparison with a viscous system. While meteorological data were used to quantify the wind excitation and its probabilities of occurrence, assumptions were made on the possible effects of motion on employees as a function of the acceleration levels. Simulation results showed that the HPCS significantly outperformed the viscous system when the effects of motion were substantial at higher wind speeds, attributed to the better performance of the HPCS at higher wind levels. The HPCS performed similarly to the viscous system, yet slightly better, when fewer employees were assumed to be affected by higher acceleration levels.

This preliminary investigation demonstrated that the proposed PBD procedure is promising at estimating the potential economic benefits of a HPCS. Future work will include possible design alterations in the control loop, and refinement of estimations on probabilities.

ACKNOWLEDGEMENT

This material is based upon work supported by the National Science Foundation under Grants No. 1463252 and 1537626. Their support is gratefully acknowledged. Any opinions, findings, and conclusions or recommendations expressed in this material are those of the authors and do not necessarily reflect the views of the National Science Foundation.

REFERENCES

[1] Connor, J. J. and Laflamme, S., [*Structural Motion Engineering*], Springer (2014).

[2] Spencer Jr, B. and Nagarajaiah, S., "State of the art of structural control," *Journal of Structural Engineering* **129**, 845 (2003).

[3] Ubertini, F., Comanducci, G., and Laflamme, S., "A parametric study on reliability-based tuned-mass damper design against bridge flutter," *Journal of Vibration and Control* (2015).

[4] Ubertini, F., "Prevention of suspension bridge flutter using multiple tuned mass dampers," *Wind and Structures* **13**(3), 235–256 (2010).

[5] Cao, L., Downey, A., Laflamme, S., Taylor, D., and Ricles, J., "Variable friction device for structural control based on duo-servo vehicle brake: Modeling and experimental validation," *Journal of Sound and Vibration* **348**, 41–56 (2015).

[6] Downey, A., Cao, L., Laflamme, S., Taylor, D., and Ricles, J., "High capacity variable friction damper based on band brake technology," *Engineering Structures* **113**, 287–298 (2016).

[7] Cao, L., Laflamme, S., Taylor, D., and Ricles, J., "Simulations of a variable friction device for multihazard mitigation," *Journal of Structural Engineering* **142**(12), H4016001 (2016).

[8] Irwin, P., Kilpatrick, J., Robinson, J., and Frisque, A., "Wind and tall buildings: negatives and positives," *The structural design of tall and special buildings* **17**(5), 915–928 (2008).

[9] Jackson, M. and Scott, D. M., "Increasing efficiency in tall buildings by damping," in [*Structures Congress 2010*], 3132–3142 (2010).

[10] Taflanidis, A. and Gidaris, I., "Life-cycle cost based optimal retrofitting of structures by fluid dampers," in [*Structures Congress 2013: Bridging Your Passion with Your Profession*], 1777–1788 (2013).

[11] Sarkisian, M., Lee, P., Hu, L., Garai, R., Tsui, A., and Reis, E., "Achieving enhanced seismic design using viscous damping device technologies," in [*Structures Congress 2013: Bridging Your Passion with Your Profession*], 2729–2744 (2013).

[12] Laflamme, S., Taylor, D., Abdellaoui Maane, M., and Connor, J. J., "Modified friction device for control of large-scale systems," *Structural control and health monitoring* **19**(4), 548–564 (2012).

[13] Alipour, A., Shafei, B., and Shinozuka, M., "Performance evaluation of deteriorating highway bridges located in high seismic areas," *Journal of Bridge Engineering* **16**(5), 597–611 (2010).

[14] Cui, W. and Caracoglia, L., "Simulation and analysis of intervention costs due to wind-induced damage on tall buildings," *Engineering Structures* **87**, 183–197 (2015).
[15] Takahashi, Y., Kiureghian, A. D., and Ang, A. H.-S., "Life-cycle cost analysis based on a renewal model of earthquake occurrences," *Earthquake engineering & structural dynamics* **33**(7), 859–880 (2004).
[16] Wen, Y. and Shinozuka, M., "Cost-effectiveness in active structural control," *Engineering structures* **20**(3), 216–221 (1998).
[17] Hahm, D., Ok, S.-Y., Park, W., Koh, H.-M., and Park, K.-S., "Cost-effectiveness evaluation of an mr damper system based on a life-cycle cost concept," *KSCE Journal of Civil Engineering* **17**(1), 145–154 (2013).
[18] Gidaris, I. and Taflanidis, A., "Design of fluid viscous dampers for optimal life cycle cost," in [*Proceedings of 15th world conference of earthquake engineering, Lisbon, Portugal*],
[19] Burns, S. A., [*Recent advances in optimal structural design*], ASCE Publications (2002).
[20] Ellingwood, B. R., Rosowsky, D. V., Li, Y., and Kim, J. H., "Fragility assessment of light-frame wood construction subjected to wind and earthquake hazards," *Journal of Structural Engineering* **130**(12), 1921–1930 (2004).
[21] Petrini, F. and Ciampoli, M., "Performance-based wind design of tall buildings," *Structure and Infrastructure Engineering* **8**(10), 954–966 (2012).
[22] Bobby, S., Spence, S. M., Bernardini, E., and Kareem, A., "Performance-based topology optimization for wind-excited tall buildings: A framework," *Engineering Structures* **74**, 242–255 (2014).
[23] ASCE, *Minimum Design Loads for Buildings and Other Structures: ASCE Standard 7-10* (American Society of Civil Engineers, Reston, VA., 2010).
[24] Lamb, S., Kwok, K. C., and Walton, D., "A longitudinal field study of the effects of wind-induced building motion on occupant wellbeing and work performance," *Journal of wind engineering and industrial aerodynamics* **133**, 39–51 (2014).
[25] Lamb, S. and Kwok, K., "Sopite syndrome in wind-excited buildings: productivity and wellbeing impacts," *Building Research & Information* , 1–12 (2016).
[26] Griffis, L. G., "Serviceability limit states under wind load," *Engineering journal/American institute of steel construction* (2003).
[27] Mendis, P., Ngo, T., Haritos, N., Hira, A., Samali, B., and Cheung, J., "Wind loading on tall buildings," *EJSE Special Issue: Loading on Structures* **3**, 41–54 (2007).
[28] Mardfekri, M. and Gardoni, P., "Multi-hazard reliability assessment of offshore wind turbines," *Wind Energy* **18**(8), 1433–1450 (2015).
[29] Laflamme, S. et al., *Control of large-scale structures with large uncertainties*, PhD thesis, Massachusetts Institute of Technology (2011).
[30] McNamara, R. and Taylor, D., "Fluid viscous dampers for high-rise buildings," *The Structural Design of Tall and Special Buildings* **12**(2), 145–154 (2003).
[31] Deodatis, G., "Simulation of ergodic multivariate stochastic processes," *Journal of engineering mechanics* **122**(8), 778–787 (1996).
[32] Chen, X. and Kareem, A., "Proper orthogonal decomposition-based modeling, analysis, and simulation of dynamic wind load effects on structures," *Journal of Engineering Mechanics* **131**(4), 325–339 (2005).
[33] Li, G. and Hu, H., "Risk design optimization using many-objective evolutionary algorithm with application to performance-based wind engineering of tall buildings," *Structural Safety* **48**, 1–14 (2014).
[34] "National occupational employment and wage estimates united states," *United States Department of Labor* (2015).
[35] NOAA, "National oceanic and atmospheric administration, station 44013, boston 16 nm east of boston, ma."